Kinetic Analysis of Smad Nucleocytoplasmic Shuttling Reveals a Mechanism for Transforming Growth Factor β-Dependent Nuclear Accumulation of Smads†

Bernhard Schmierer and Caroline S. Hill*

Laboratory of Developmental Signalling, Cancer Research UK London Research Institute, 44 Lincoln's Inn Fields, London WC2A 3PX, United Kingdom

Upon transforming growth factor β (TGF-β) stimulation, Smads accumulate in the nucleus, where they regulate gene expression. Using fluorescence perturbation experiments on Smad2 and Smad4 fused to either enhanced green fluorescent protein or photoactivatable green fluorescent protein, we have studied the kinetics of Smad nucleocytoplasmic shuttling in a quantitative manner in vivo. We have obtained rate constants for import and export of Smad2 and show that the cytoplasmic localization of Smad2 in uninduced cells reflects its nuclear export being more rapid than import. We find that TGF-β-induced nuclear accumulation of Smad2 is caused by a pronounced drop in the export rate of Smad2 from the nucleus, which is associated with a strong decrease in nuclear mobility of Smad2 and Smad4. TGF-β-induced nuclear accumulation involves neither a release from cytoplasmic retention nor an increase in Smad2 import rate. Hence, TGF-β-dependent nuclear accumulation of Smad2 is caused exclusively by selective nuclear trapping of phosphorylated, complexed Smad2. The proposed mechanism reconciles signal-dependent nuclear accumulation of Smad2 with its continuous nucleocytoplasmic cycling properties.

Signals from transforming growth factor β (TGF-β) receptors are transduced to the nucleus by members of the Smad family. Upon TGF-β signaling, the receptor-regulated Smads (R-Smads), Smad2 and Smad3, are phosphorylated by the type I receptor, allowing them to form complexes with Smad4. These complexes accumulate in the nucleus, where they are directly involved in gene regulation (17). The R-Smads also form homomeric complexes in response to TGF-β that accumulate in the nucleus, but their role in gene regulation is not entirely clear.

Although TGF-β signaling leads to a change in overall Smad distribution from predominantly cytoplasmic to predominantly nuclear, recent work has indicated that these distributions are not static. Rather, they represent two different steady states of a dynamic equilibrium. The Smads shuttle continuously between the cytoplasm and nucleus in unstimulated cells (7, 10, 13, 20, 26, 27), and also in the presence of a TGF-β signal, even at maximal nuclear accumulation (7). In the presence of TGF-β, R-Smads and Smad4 are exported from the nucleus independently of each other, and the R-Smads that appear in the cytoplasm are unphosphorylated (7, 26). This suggests that Smad complexes disassemble in the nucleus, probably following R-Smad dephosphorylation by an as yet unidentified phosphatase (7).

Export of Smad4 from the nucleus is CRM-1 dependent and can be blocked by leptomycin B (LMB) (13, 20). Moreover, Smad4 export has recently been shown to be inhibited by complex formation with activated Smad3, providing further evidence that Smad complexes have to dissociate in the nucleus to allow monomeric Smads to be exported (2). R-Smad export is independent of CRM-1, and no transport receptor has been identified. It is thought that R-Smad export may simply be mediated by direct interactions with nucleoporins (24, 26, 27). Import of Smad3 and Smad4 is thought to be importin β dependent (8, 22, 23). However, Smad2, Smad3, and Smad4 have also been proposed to enter the nucleus by direct interactions with the nuclear pore complex, avoiding the need for a soluble transport receptor (24, 26, 27).

Inhibition of the type I receptor in TGF-β-treated cells that have reached maximal accumulation causes R-Smads to relocalize to the cytoplasm, indicating that continuous receptor activity is required for sustained nuclear localization of the Smads even after the initial accumulation phase (7). Such sustained nuclear localization of Smads is required for induction or repression of a subset of Smad-responsive genes, and thus the time period for which the Smads stay nuclear is considered a major determinant of the readout of TGF-β signaling (11). Despite their crucial importance for a quantitative understanding of the signaling pathway, the mechanisms that govern the subcellular localization of Smads in unstimulated cells, the kinetics of TGF-β-dependent Smad nuclear accumulation, maintenance of Smad nuclear localization, and Smad relocalization to the cytoplasm after prolonged signaling are largely unknown.

The central questions we have addressed here concern how the predominant cytoplasmic localization of Smads in uninduced cells is determined and how TGF-β brings about nuclear accumulation of Smads, given their continuous exchange between the nuclear and the cytoplasmic pools in both uninduced and induced cells. We have combined conventional photobleaching techniques with a novel photoactivation approach

---

* Corresponding author. Mailing address: Cancer Research UK London Research Institute, 44 Lincoln's Inn Fields, London WC2A 3PX, United Kingdom. Phone: 44-20-7269-2941. Fax: 44-20-7269-3093. E-mail: Caroline.Hill@cancer.org.uk.

(12), to obtain quantitative information about the mechanisms that establish nucleocytoplasmic distribution of Smad2 and Smad4 in vivo in both TGF-β-induced and in uninduced cells. Photoactivatable green fluorescent protein (PAGFP) is a point-mutated variant of enhanced green fluorescent protein (EGFP) that, after short exposure to light of wavelength of 413 nm, immediately increases fluorescence approximately 100 times when excited with 488 nm light (12).

PAGFP-Smad fusions were photoactivated specifically in the nucleus or cytoplasm by focal plane-restricted multiphoton excitation to enable us to study, for the first time, Smad export and import independently of each other. This approach was complemented with photobleaching experiments using EGFP-Smad fusions. We have obtained nuclear import and export rate constants for Smad2 in uninduced cells and demonstrate that the predominantly cytoplasmic localization of Smad2 in uninduced cells results from its export being faster than its import. We demonstrate that the well-conserved N-terminal MH1 domain (17) plays an important role in this. We show that Smad nuclear accumulation upon TGF-β signaling is caused by a pronounced decrease in nuclear export of TGF-β-activated Smads, which is accompanied by a significant decrease in Smad mobility in the nucleus. We find no evidence for a TGF-β-dependent increase in Smad nuclear import rate, or for a TGF-β-dependent release of Smads from cytoplasmic anchoring. Our data indicate that Smad2 phosphorylation by the receptor kinase or upstream events such as presentation of R-Smads to the receptors are the rate-limiting steps in the nuclear accumulation process and we propose a model in which the nucleus acts as a trap, filtering activated Smad complexes out of the total shuttling pool of monomeric Smads.

MATERIALS AND METHODS

Plasmids, reagents, and cell lines. Plasmids expressing EGFP-Smads and hemagglutinin (HA)-tagged *Xenopus* FoxH1 were previously described (10, 15). Plasmids expressing PAGFP-Smads were generated from the EGFP-Smad constructs by swapping the EGFP for PAGFP from pPAGFP-C1 (a gift from George Patterson and Jennifer Lippincott-Schwartz). EGFP-Smad2 ΔMH1 corresponded to a fusion of EGFP with Smad2 residues 198 to 467. EGFP-Smad2 W368A and D300H were generated from EGFP-Smad2 by PCR. All constructs were sequenced.

TGF-β (PeproTech) was used at a final concentration of 2 ng/ml. SB-431542 (Tocris) was used at a final concentration of 10 μM and LMB (Calbiochem) at 20 ng/ml. Cell lines stably expressing GFP-Smads and unfused PAGFP were generated by transfecting HaCaT cells with the appropriate plasmids using Fu-GENE 6 (Roche) and selecting transfected cells using 1 mg/ml G418 (Invitrogen). For wild-type GFP-Smads and unfused PAGFP, positive single-cell clones were expanded and analyzed for GFP-Smad expression by fluorescence microscopy. Routine cell culture following selection was performed in Dulbecco's modified Eagle's medium with 10% fetal bovine serum containing 500 μg/ml G418. Mutant EGFP-Smad2 cell lines were generated as above, but in these cases pools of expressing cells were generated using fluorescence-activated cell sorting. HeLa TK⁻ cells (1) were grown in Dulbecco's modified Eagle's medium with 10% fetal bovine serum and the cell line expressing EGFP-Smad2 was generated as for HaCaT cells. They were transfected using Lipofectamine 2000 (Invitrogen).

Immunoblotting and immunoprecipitation. Whole-cell extracts were prepared as previously described (4) and immunoblotting was performed using standard techniques with monoclonal anti-Smad2/3 (BD Biosciences), anti-Smad4 (B8; Santa Cruz), and anti-GFP (CR-UK), and polyclonal anti-phosphorylated Smad2 (Cell Signaling Technology) antibodies. Band intensities on immunoblots were quantitated using the ImageJ 1.32j software. Immunoprecipitation was performed with anti-GFP (Roche) in immunoprecipitation buffer (50 mM Tris-HCl, pH 7.4, 150 mM NaCl, 1 mM EDTA, 1% NP-40, 0.25% sodium deoxy-cholate, phosphatase inhibitors, and protease inhibitors).

Confocal microscopy. Microscopy was performed using an LSM 510 confocal microscope (Zeiss) equipped with an Argon Laser and a Mira 900 multiphoton titanium-sapphire laser (Coherent). Imaging of EGFP as well as PAGFP after photoactivation was performed with a Plan Apochromat 63x 1.4 NA oil immersion objective using 488-nm excitation and collecting emission using a 500 to 550-nm bandpass filter. Settings were adjusted such that photobleaching due to image acquisition was negligible in all experiments. Images were acquired using the microscope software (Zeiss). Cells were plated onto coverslips 20 to 40 h before the experiment in microscopy medium (low bicarbonate culture medium minus phenol red containing 2.2 g/liter NaHCO₃ and 25 mM HEPES, pH 7.4). All live cell imaging was performed at 37°C.

Photoactivation. Photoactivation of the PAGFP moiety was carried out with the multiphoton laser (approximately 600-mW output) tuned to a wavelength of 820 nm, which approximates 410-nm multiphoton excitation in the focal plane, using the bleaching protocol of the confocal software. The activation region was chosen to include the whole compartment to be activated (cytoplasm or nucleus) and was scanned with 90% laser power for between 5 and 20 seconds, resulting in activation of PAGFP. Images were then acquired as above.

Determination of first-order rate constants of import and export. Entire nuclei of EGFP-Smad cell lines were photobleached for 5 seconds with 100% laser power (488 nm). Alternatively, the entire cytoplasm of PAGFP-expressing cells was photoactivated for the same time. The appearance of nuclear fluorescence and loss of cytoplasmic fluorescence were monitored until the establishment of a steady state. At each time point, nuclear and cytoplasmic fluorescence were normalized to whole-cell fluorescence. Nuclear fluorescence directly after the fluorescence perturbation was set to zero; cytoplasmic fluorescence directly after perturbation was set to 1. Assuming first-order kinetics for both import and export, a model equation for the increase in nuclear fluorescence was derived (see Fig. S1 in the supplemental material). The experiments were performed on 10 cells for each protein studied and the obtained values for import rate constants, export rate constants, and for the ratio of cytoplasmic to nuclear volume were averaged.

Initial export rates. Entire nuclei of PAGFP-Smad cell lines treated for 1 h with SB-431542, TGF-β, or LMB were photoactivated as described above and fluorescence loss due to export was monitored for 60 seconds after activation. Values were corrected for background and normalized to the nuclear fluorescence directly after photoactivation. At early time points, curves could be approximated accurately by an exponential decrease, yielding an initial export rate.

Initial import rates. Entire nuclei of EGFP-Smad cell lines were photobleached with 100% laser power (488 nm) and appearance of nuclear fluorescence was monitored. Nuclear fluorescence directly after bleaching was set to zero and the subsequent nuclear fluorescence values were normalized to the whole-cell fluorescence prior to bleaching. Initial import rates were measured in SB-431542-treated cells or cells treated with TGF-β for 10 to 40 min, i.e., during the actual accumulation phase. Long term import experiments were performed in SB-431542-treated cells and in TGF-β-treated cells after establishment of maximal nuclear accumulation of Smads.

Fluorescence recovery after photobleaching data acquisition. Ten prebleach pictures were taken at 0.1% laser power, then a rectangular bleach area of 2.9 μm width crossing either a whole nucleus or the whole cytoplasm was scanned 54 times with 100% laser power, giving rise to a bleaching time of 500 ms. Directly after the bleach, 300 images were taken at 200-ms intervals at a size of 256 by 256 pixels, corresponding to an optical field of 73 by 73 μm.

Fluorescence recovery after photobleaching data analysis. Fluorescence of the bleach region and of the entire compartment were both corrected for background and normalized to the average prebleach fluorescence in the corresponding region (single normalization). Further normalization was performed by dividing the background-corrected single-normalized fluorescence of the bleach region by the background-corrected single normalized fluorescence of the entire compartment. Data from 10 cells were pooled into an average recovery curve, which was then further normalized such that the initial fluorescence after the bleach was set to zero and full recovery was set to 1. Recovery half-times were obtained by linear interpolation between the data points immediately above and below 50% recovery.

RESULTS

HaCaT cell lines express tagged Smads at endogenous levels. HaCaT cells are immortalized human keratinocytes, which exhibit an epithelial morphology and show strong nuclear accumulation of activated Smads and highly regulated Smad-dependent transcription, indicating a robust TGF-β response
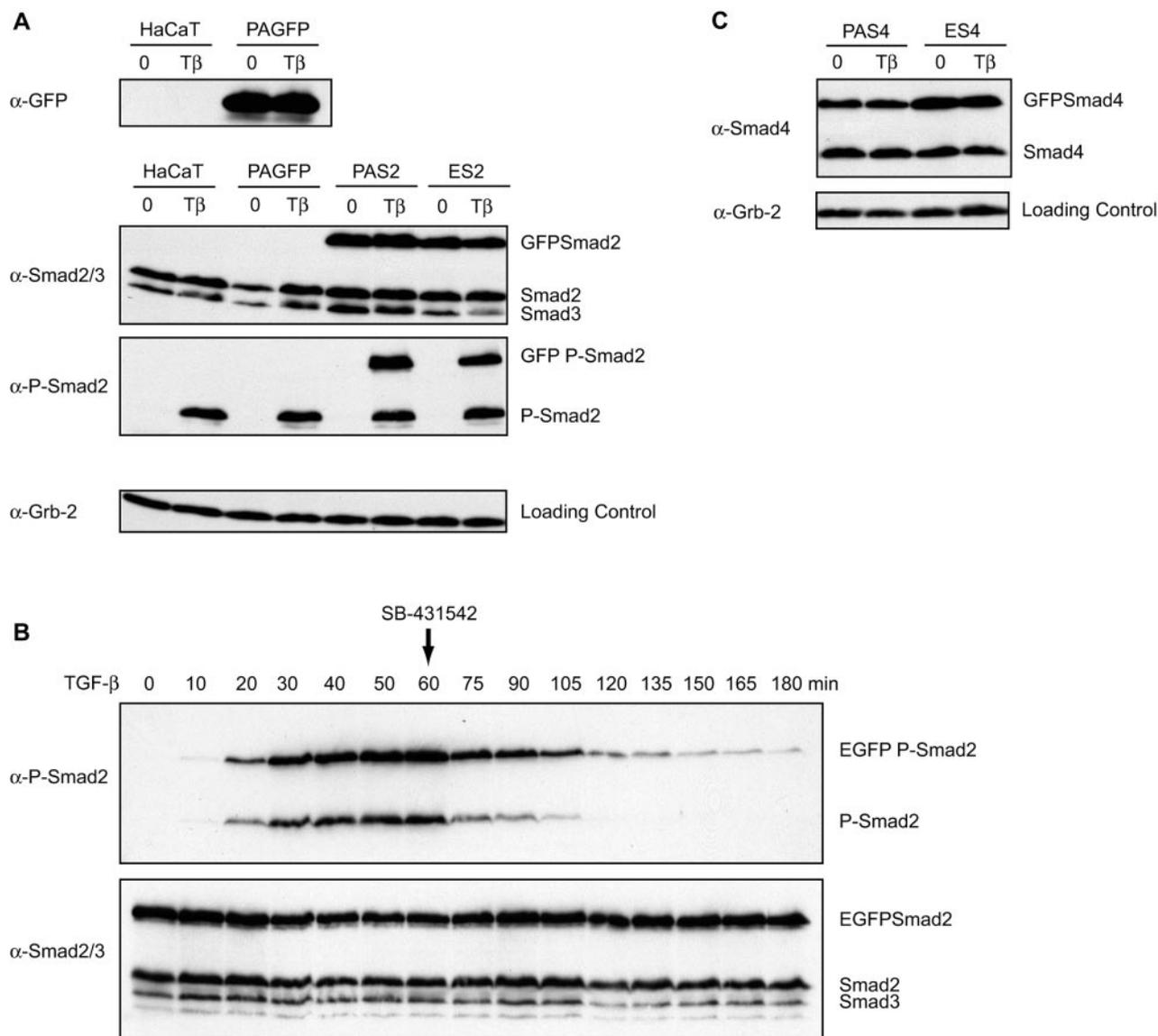
FIG. 1. Characterization of the cell lines used. Whole-cell extracts were subjected to immunoblotting with antibodies as indicated. A. Parental cells (HaCaT) and cell lines expressing PAGFP (PAGFP), PAGFP-tagged Smad2 (PAS2) and EGFP-tagged Smad2 (ES2). PAGFP alone is highly expressed, PAGFP-Smad2 and EGFP-Smad2 are both expressed at levels comparable to endogenous Smad2 and are readily phosphorylated in response to 1 h treatment with 2 ng/ml TGF-β (Tβ). B. EGFP-Smad2 phosphorylation exhibits a very similar kinetics as endogenous Smad2 phosphorylation in response to TGF-β. Upon addition of SB-431542 to cells that have been pretreated with TGF-β, EGFP-Smad2 and endogenous Smad2 become dephosphorylated with highly similar kinetics. C. Cell lines expressing PAGFP-Smad4 (PAS4) and EGFP-Smad4 (ES4). Both proteins are expressed at approximately endogenous levels.

(11, 13). We have established clonal HaCaT cell lines expressing Smad2 and Smad4 fused to EGFP, as well as HaCaT cell lines expressing these Smads fused to PAGFP. N-terminal tagging with GFP does not interfere with localization or function of either Smad2 or Smad4 (10). Importantly the HaCaT cell lines used in this study express the GFP-Smad fusions at approximately endogenous levels (Fig. 1A and C).

Both EGFP-Smad2 and PAGFP-Smad2 are readily phosphorylated in response to TGF-β (Fig. 1A), and both are phosphorylated with very similar kinetics to endogenous Smad2 (Fig. 1B; data not shown). Upon addition of the highly specific TGF-β type I receptor inhibitor SB-431542 (6, 9),

phosphorylated EGFP-Smad2 and phosphorylated PAGFP-Smad2 start to become dephosphorylated immediately (Fig. 1B and data not shown). Quantitative densitometric analysis of different exposure times revealed that the dephosphorylation kinetics of GFP-tagged Smad2 is very similar to the dephosphorylation kinetics of endogenous Smad2 (Fig. 1B and data not shown). These HaCaT cell lines are particularly well suited for studying intracellular protein distribution in a quantitative manner, because their moderate expression of the transgenes avoids problems such as aberrant subcellular localization due to substantial overexpression, which is frequently seen in transiently transfected cells (data not shown). Moreover, HaCaT

cell lines show barely any autocrine TGF-β signaling (Fig. 1B, first lane). As a precaution though, all control experiments have been routinely performed in the presence of SB-431542 to exclude any autocrine TGF-β signaling. The behavior of untreated cells however did not differ significantly from SB-431542-treated cells (data not shown). A cell line expressing the freely diffusible unfused PAGFP was used as a control (Fig. 1A).

Photoactivation provides direct visual proof of Smad2 nucleocytoplasmic shuttling. To visualize Smad2 shuttling in uninduced cells in real time, HaCaT cells stably expressing PAGFP-Smad2 were treated with SB-431542 and PAGFP-Smad2 was then photoactivated either in the nucleus (Fig. 2Ai) or in the cytoplasm (Fig. 2Bi). Significant amounts of photoactivated PAGFP-Smad2 appeared in the other compartment within a few minutes. Note that the weak fluorescence in Fig. 2Ai is due to the low amounts of PAGFP-Smad2 that are present in the nucleus of unstimulated cells. Irrespective of which compartment had been photoactivated, PAGFP-Smad2 rapidly attained a steady-state distribution typical for uninduced cells, with photoactivated PAGFP-Smad2 being predominantly cytoplasmic. This experiment proves that there is a dynamic equilibrium between nuclear and cytoplasmic PAGFP-Smad2, and provides direct visual proof that Smad2 is shuttling between both compartments in the absence of a TGF-β signal.

When the same experiment was performed in cells that had been induced with TGF-β for 1 h to yield maximal Smad nuclear accumulation (7), similar results were obtained. As expected, PAGFP-Smad2 photoactivated in the nucleus appeared in the cytoplasm (Fig. 2Aii) and when PAGFP-Smad2 was photoactivated in the cytoplasm, it appeared in the nucleus (Fig. 2Bii). Importantly, photoactivated PAGFP-Smad2 again attained the expected steady-state distribution, in this case predominantly nuclear, regardless of which compartment had been photoactivated. This experiment directly proves that in the presence of TGF-β, even at maximal nuclear accumulation, Smad2 is continuously shuttling between the cytoplasm and nucleus.

There is no substantial cytoplasmic pool of phosphorylated Smad2. Smad2 is trickling in and out of the nucleus even in cells that have reached maximal nuclear accumulation. How is nuclear accumulation maintained for several hours under these circumstances? Two possible mechanisms can be envisaged to explain sustained nuclear accumulation of Smad2 despite continuous exchange with the cytoplasmic pool. Cytoplasmic and nuclear pools of phosphorylated Smad2 could exist, which are in dynamic equilibrium with each other. Alternatively, sustained nuclear accumulation of Smad2 could require cycles of Smad2 phosphorylation and dephosphorylation.

To distinguish between these possibilities we asked whether sustained nuclear accumulation of Smad2 still required receptor-induced Smad2 phosphorylation. PAGFP-Smad2-expressing cells were pretreated with TGF-β until a steady state of maximal Smad2 nuclear accumulation was reached. Then, SB-431542 was added to inhibit TGF-β type I receptor activity (6). After 10 min of SB-431542 treatment, to ensure the receptors were completely inactivated, the cytoplasm was photoactivated. If a cytoplasmic pool of activated complexes existed, we should detect substantial nuclear import of photoactivated cytoplasmic PAGFP-Smad2 under these conditions, similar to

that seen in TGF-β-induced cells (Fig. 2Bii). However, only a small amount of PAGFP-Smad2 appeared in the nucleus (Fig. 2Biii). The cytoplasmically photoactivated PAGFP-Smad2 remained mainly cytoplasmic, attaining a distribution similar to a cell that had never been exposed to TGF-β. Thus, the strong nuclear accumulation of cytoplasmically photoactivated PAGFP-Smad2 seen in TGF-β-induced cells (Fig. 2Bii) only occurs when receptors are continuously active, suggesting that such accumulation represents de novo phosphorylated PAGFP-Smad2 replacing "invisible" nuclear phosphorylated PAGFP-Smad2. Hence, maintenance of nuclear accumulation of Smad2 requires cycles of Smad2 phosphorylation and dephosphorylation and the steady state of maximal nuclear accumulation does not simply reflect the nucleocytoplasmic distribution of phosphorylated Smad2. We infer from this and other evidence (see Discussion) that there is no substantial, long-lived pool of phosphorylated Smad2 in the cytoplasm in TGF-β-induced cells.

The absence of a substantial, long-lived pool of phosphorylated Smad2 in the cytoplasm suggests that the processes leading to Smad2 phosphorylation are rate limiting for nuclear accumulation of phosphorylated Smad2 and that the translocation step is relatively fast compared to receptor-dependent Smad2 phosphorylation. Consistent with this idea, Smad2 phosphorylation proceeds with highly similar kinetics to Smad2 accumulation, both reaching a maximum after about 45 min of TGF-β treatment (Fig. 1B) (see references 7 and 10).

Smad2 export is more rapid than import in unstimulated cells. We next addressed the mechanism underlying the steady-state distribution of Smad2 in unstimulated cells by following the kinetics of EGFP-Smad2 nucleocytoplasmic shuttling. Nuclei of EGFP-Smad2-expressing cells were photobleached and the rate of reappearance of EGFP-Smad2 in the nucleus as well as the rate of disappearance of EGFP-Smad2 from the cytoplasm was measured (Fig. 3Ai). The obtained curves could be readily fitted to a first-order model equation, which was derived by assuming first-order kinetics for both import and export. We thus conclude that in unstimulated cells, the cytoplasmic and nuclear concentrations of EGFP-Smad2 are the predominant rate limiting factors for import and export, respectively. Fitting the model equation to the data yielded values for the first-order import and export rate constants k_{imp} and k_{exp}, as well as for the volume ratio between cytoplasm and nucleus (A) for each individual cell. For details refer to Materials and Methods and Fig. S1 in the supplemental material. For EGFP-Smad2, we measured an import rate constant of 0.0027 ± 0.0004 s^{-1} and an export rate constant of 0.0058 ± 0.0007 s^{-1} (Fig. 3B). The observation that the export rate constant exceeds the import rate constant explains why the EGFP-Smad2 is predominantly cytoplasmic in the absence of a TGF-β signal.

We have observed that the subcellular localization of EGFP-Smad2 with its N-terminal MH1 domain (17) deleted (EGFP-Smad2 ΔMH1) differs from that of wild-type Smad2, in that it is substantially nuclear in unstimulated cells (Fig. 3Aii). As for full-length EGFP-Smad2, nucleocytoplasmic shuttling of the truncated protein could be approximated by first-order kinetics. We found that EGFP-Smad2 ΔMH1 shuttled between the cytoplasm and nucleus much more rapidly than full-length EGFP-Smad2 and both its import and export rate constants
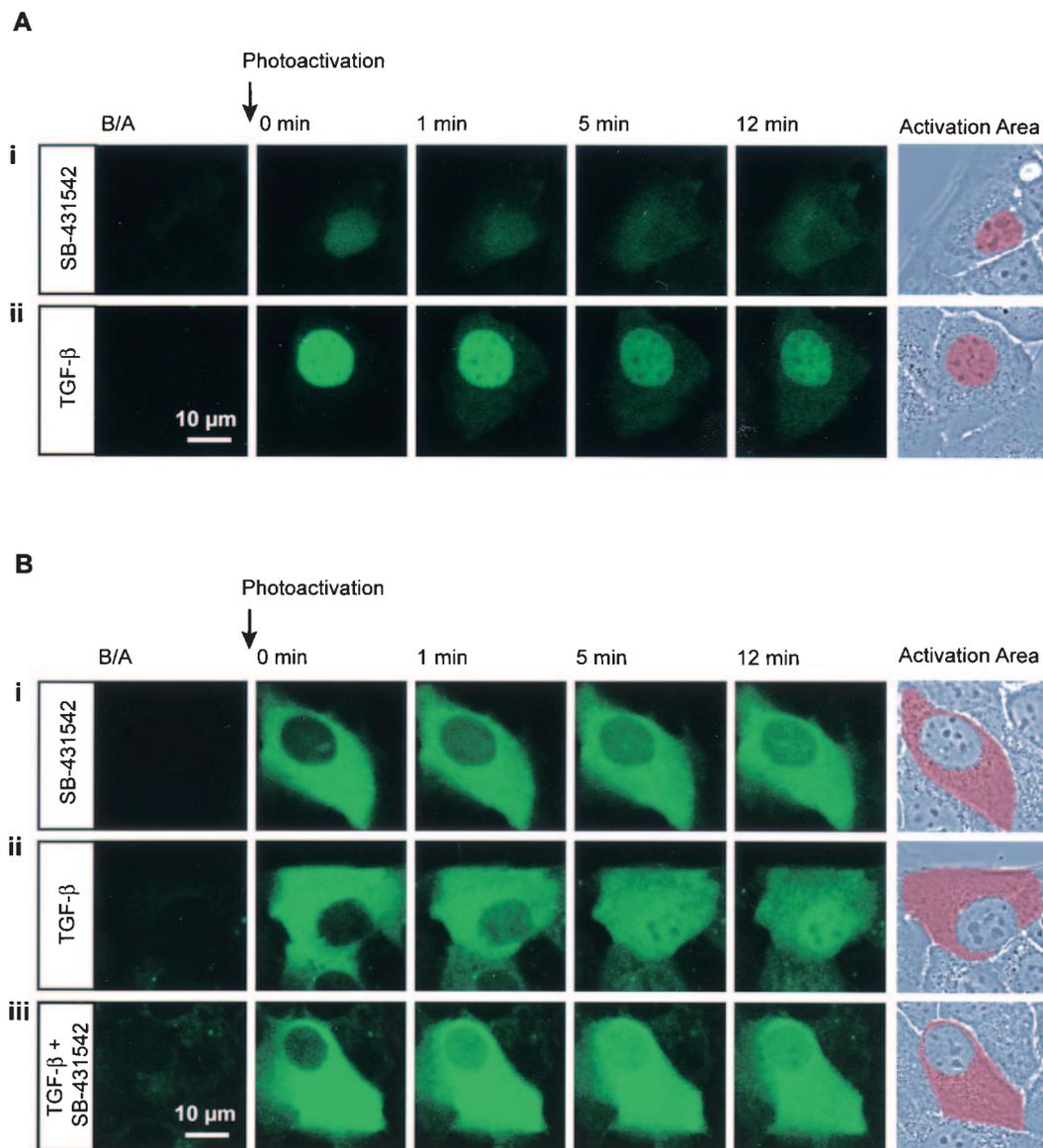
FIG. 2. Compartment-specific photoactivation of PAGFP-Smad2. Cells are shown directly before photoactivation (B/A), and 0, 1, 5, and 12 min after a 10- to 20-second photoactivation of a specific compartment. The shaded area in the phase contrast pictures indicates the actual photoactivation area. A. Nuclear photoactivation of PAGFP-Smad2 by repeatedly scanning an area containing the nucleus in cells treated for 15 min with SB-431542 (i) or cells induced for 1 h with TGF-β (ii). In SB-431542-treated cells, PAGFP-Smad2 photoactivated in the nucleus accumulates in the cytoplasm, reaching a distribution typical for an uninduced cell. Despite strong nuclear accumulation in TGF-β-treated cells, a significant proportion of PAGFP-Smad2 becomes visible in the cytoplasm with increasing time. B. Cytoplasmic photoactivation by scanning an area comprising the whole cytoplasm but excluding the nucleus. (i) SB-431542-treated cells quickly reach a steady-state distribution typical for uninduced cells. In TGF-β-treated cells, which have reached a state of maximal accumulation prior to photoactivation, cytoplasmically photoactivated PAGFP-Smad2 still accumulates in the nucleus, provided the receptors are active (ii), but not if receptors have been inactivated by SB-431542 added 90 min after the TGF-β and 10 min before photoactivation (iii). Pictures show representatives from at least 3 independent experiments.

were substantially higher than those obtained for full-length EGFP-Smad2 (Fig. 3B).

To exclude the possibility that the higher shuttling speed of EGFP-Smad2 ΔMH1 was due to its smaller size, we followed the shuttling kinetics of unfused GFP by activating the cytoplasm of cells expressing unfused PAGFP and measuring its appearance in the nucleus and its loss from the cytoplasm (Fig. 3Aiii). Import and export rate constants for unfused PAGFP were significantly lower than for EGFP-Smad2 ΔMH1 (Fig.

3B). Thus, EGFP-Smad2 ΔMH1 (~60 kDa) is actually shuttling much more rapidly than the much smaller PAGFP (~30 kDa) and the difference between EGFP-Smad2 ΔMH1 and full-length EGFP-Smad2 (~80 kDa) cannot be explained by the size difference. Rather, our results indicate that the MH1 domain acts to restrict both nuclear import and export of Smad2. Because its effect on import is more profound, the MH1 domain is responsible for the predominantly cytoplasmic localization of Smad2 in unstimulated cells.
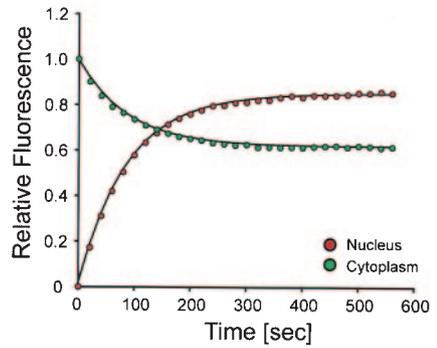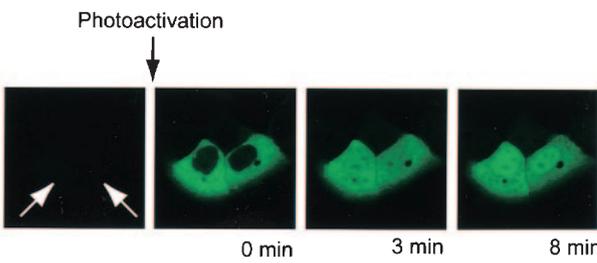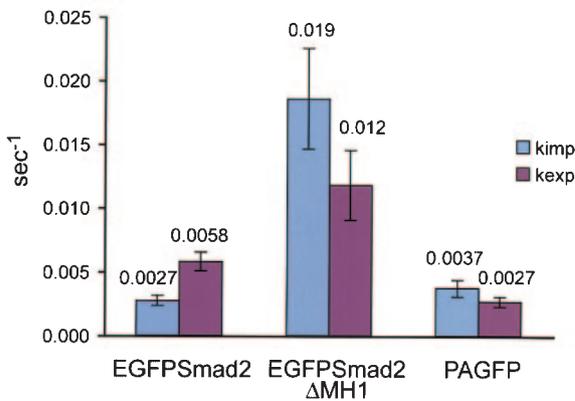
A

i) EGFPSmad2
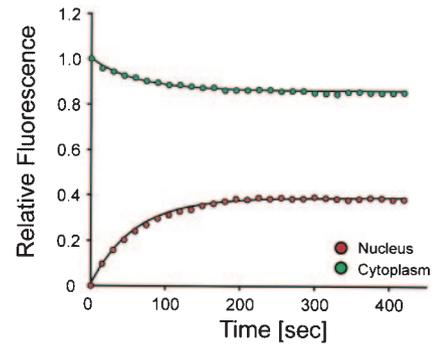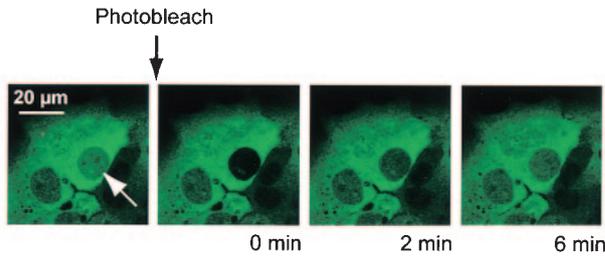
ii) EGFPSmad2 ΔMH1
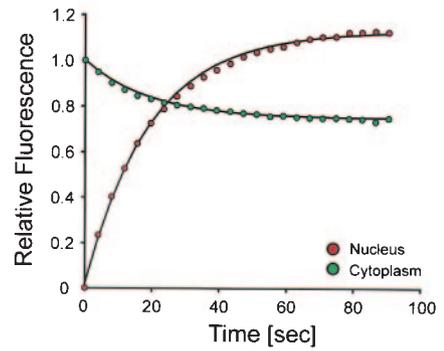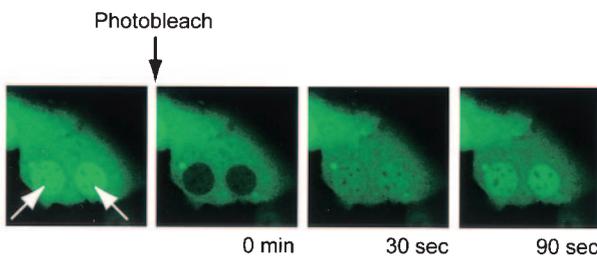
iii) PAGFP

B   Import and export rate constants

Quantification of Smad redistribution upon TGF-β signaling. Having established that the predominantly cytoplasmic localization of Smad2 in uninduced cells is due to nuclear export being faster than nuclear import, we asked what TGF-β-induced Smad2 phosphorylation actually does to shift Smad2 from a predominantly cytoplasmic towards a mainly nuclear localization, given its continuous nucleocytoplasmic cycling properties.

To begin to answer this important question, we first determined the relative amounts of Smad2 that actually redistribute into the nucleus in response to TGF-β. To this end, we measured the ratio of mean nuclear fluorescence to mean cytoplasmic fluorescence (R) in EGFP-Smad-expressing HaCaT cells in the absence or presence of TGF-β (Fig. 4A). This is equivalent to the ratio of nuclear to cytoplasmic EGFP-Smad2 concentrations. In uninduced cells, R was equal to 0.53 ± 0.08 (Fig. 4B), which is in very good agreement with the value derived from the kinetic analysis shown in Fig. 3, where R is equal to $k_{imp}/k_{exp} = 0.0027/0.0058 = 0.47$. In TGF-β-induced cells, R increased to 2.5 ± 0.6 (Fig. 4B). To determine the ratio of absolute amounts of EGFP-Smad2 from the ratios of its concentrations we needed to know the average ratio of accessible cytoplasmic to accessible nuclear volume. We derived this parameter from the kinetic experiments shown in Fig. 3, and obtained an average cytoplasmic/nuclear volume ratio (A) of 2.9 ± 0.8 for HaCaT cells (see Fig. S1 in the supplemental material), which is consistent with values previously obtained for human cells (19).

From this volume ratio (A) and the ratio of nuclear to cytoplasmic fluorescence (R) (Fig. 4B), we calculated the average cytoplasmic/nuclear distribution ratio of EGFP-Smad2 in uninduced cells (A/R) to be 2.9/0.53. Hence, 15% of total EGFP-Smad2 is nuclear in uninduced cells (Fig. 4C). In TGF-β-treated cells, about 46% of total EGFP-Smad2 is nuclear (Fig. 4B). TGF-β-induced accumulation clearly requires Smad complex formation, since an EGFP-Smad2 point mutant (D300H) that is phosphorylated in response to TGF-β but fails to form Smad complexes, fails to accumulate in the nucleus upon TGF-β signaling (see Fig. S2 in the supplemental material) (21). Thus, the EGFP-Smad2 that accumulates in the nucleus in response to TGF-β consists of phosphorylated complexed EGFP-Smad2. However, there will also be a fraction of nuclear EGFP-Smad2 in TGF-β-treated cells that is unphosphorylated and monomeric and is nuclear due to constitutive shuttling. Assuming that the amount of phosphorylated EGFP-Smad2 in the cytoplasm is negligible at any time (see above) and that unphosphorylated EGFP-Smad2 will distribute identically between the cytoplasm and nucleus as it does in uninduced cells, we deduced the relative size of both fractions. In maximally accumulated cells, ~36% of the total cellular EGFP-Smad2 accumulates due to the TGF-β signal, whereas ~10% of the total cellular EGFP-Smad2 is nuclear due to constitutive shuttling (Fig. 4C). Thus, approximately 80% of nuclear EGFP-Smad2 is phosphorylated and complexed. The remainder is nuclear because of constitutive nucleocytoplasmic shuttling of the monomeric protein.

For comparison, we applied the same procedure to EGFP-Smad4-expressing cells. Of the total cellular EGFP-Smad4, ~15% accumulated in the nucleus in response to TGF-β and ~11% was nuclear due to constitutive shuttling (Fig. 4C). Weak Smad4 nuclear accumulation is expected in Smad4-overexpressing cells, since nuclear accumulation of Smad4 depends on its ability to interact with endogenous R-Smads, which will be limiting (2, 3).

TGF-β signaling decreases the export rate of Smad2. Having quantified the amount of EGFP-Smad2 being redistributed in response to TGF-β signaling, we investigated the mechanism underlying this, to determine whether it resulted from a decrease in export rate or an increase in import rate or a combination of the two. We performed photoactivation of the whole nuclear compartment in PAGFP-Smad2 cells and measured loss of nuclear fluorescence due to export during the first minute after photoactivation (Fig. 5A). At early time points after photoactivation, reimport of already exported fluorescent protein does not significantly affect nuclear fluorescence due to the small amounts exported and the dilution effect caused by the larger volume of the cytoplasm compared to the nucleus (data not shown; see Fig. 2Aii, 1-min panel). Although in the absence of TGF-β, import and export of the Smads from the nucleus obey first-order kinetics, this is not true in TGF-β-treated cells. In this case the import and export rates are no longer directly proportional to protein concentration (data not shown). Nevertheless, at these early time points, nuclear fluorescence decreases exponentially and initial export rates (expressed in % fluorescence loss from the nucleus per second) can be obtained.

In cells pretreated with TGF-β for 1 h, we observed an approximately fourfold decrease of PAGFP-Smad2 export rate compared with uninduced cells (Fig. 5A). For PAGFP-Smad4 it is clear that it is exported more slowly than PAGFP-Smad2 in uninduced cells (Fig. 5A). However, differences between export rates for PAGFP-Smad4 in TGF-β-induced and uninduced cells were not statistically significant because of the less pronounced nuclear accumulation of PAGFP-Smad4 in response to TGF-β, leading to higher noise levels. The validity of the approach was tested by taking advantage of the CRM-1-dependence of Smad4 export, which can be efficiently blocked by LMB. As expected, the presence of LMB dramatically decreased the export rate of nuclear PAGFP-Smad4 (Fig. 5A).

This key experiment demonstrates that export of nuclear

FIG. 3. Import and export rate constants. A. Nuclei of SB-431542-treated cells expressing EGFP-Smad2 (i) or EGFP-Smad2 ΔMH1 (ii) were photobleached. The reappearance of nuclear fluorescence in the nucleus and the fluorescence loss in the cytoplasm were monitored until a steady state was reached. Alternatively, the cytoplasm of untreated, PAGFP-expressing cells was photoactivated (iii) and the redistribution of fluorescence was monitored as above. In the graphs, circles represent experimental points and solid lines are theoretical curves derived from the experimental data, assuming first-order kinetics. From the curves, import rate constants and export rate constants were calculated (see Fig. S1 in the supplemental material). Pictures show representative experiments with fluorescence perturbation performed in either 1 cell (i) or two cells (ii and iii). B. Import and export rate constants obtained for EGFP-Smad2, EGFP-Smad2 ΔMH1 and PAGFP. Bars show means ± standard deviations ($n = 10$).
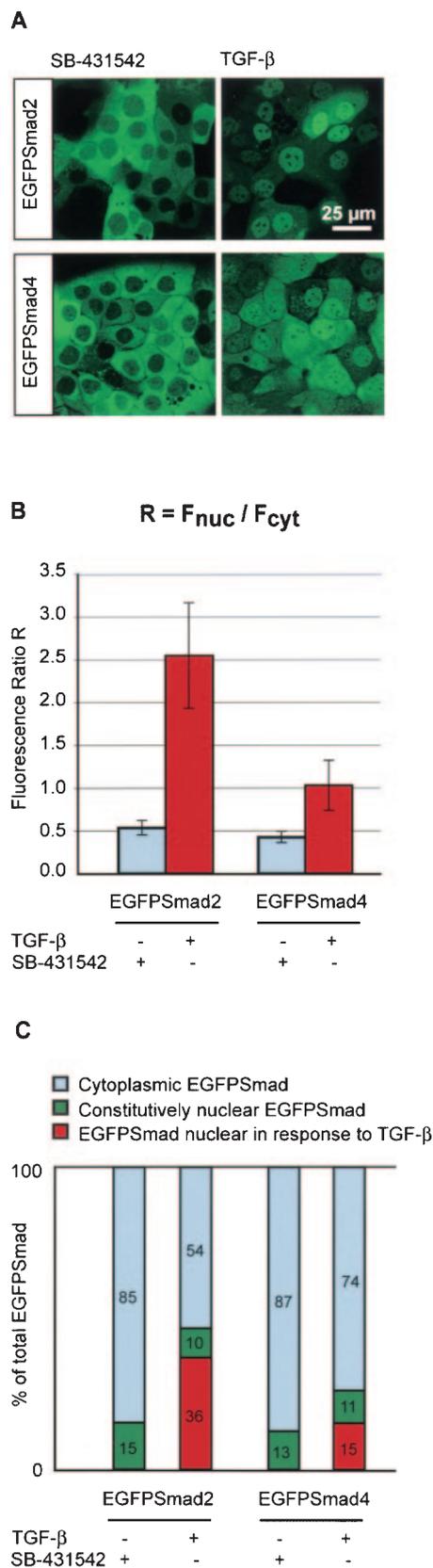
A

SB-431542   TGF-β

EGFPSmad2

EGFPSmad4

25 µm

B

$R = F_{nuc} / F_{cyt}$

Fluorescence Ratio R

EGFPSmad2   EGFPSmad4

| TGF-β | - | + | - | + |
| SB-431542 | + | - | + | - |

C

☐ Cytoplasmic EGFPSmad
☐ Constitutively nuclear EGFPSmad
☐ EGFPSmad nuclear in response to TGF-β

% of total EGFPSmad

85   54   87   74
10
15   36   13   11
           15

EGFPSmad2   EGFPSmad4

| TGF-β | - | + | - | + |
| SB-431542 | + | - | + | - |

FIG. 4. Nucleocytoplasmic distribution of EGFP-Smads in induced and uninduced cells. A. EGFP-Smad2 cells and EGFP-Smad4 cells were induced with TGF-β for 1 h or were treated with SB-431542. Pictures show representative images for each condition. B. Mean flu-

Smad2 is strongly inhibited in TGF-β-treated cells. As outlined in the previous section, in induced cells nearly 80% of nuclear EGFP-Smad2 accumulates in a TGF-β-dependent manner and is hence phosphorylated and complexed, whereas approximately 20% is nuclear due to constitutive shuttling and represents unphosphorylated, monomeric EGFP-Smad2 (Fig. 4C). The decrease in export rate that we observed can be explained if only the unphosphorylated, monomeric PAGFP-Smad2 was able to participate in export. We speculate therefore that the export observed from nuclei of TGF-β-induced cells is due to the unphosphorylated fraction of Smad2; the phosphorylated complexed Smads being trapped in the nucleus during the short time period monitored. In agreement with this notion, we found an inverse correlation between the initial export rate and the degree of Smad2 nuclear accumulation. Faster initial export rates were measured in cells that had been treated with TGF-β for shorter periods and which had consequently accumulated less phosphorylated PAGFP-Smad2 in the nucleus (data not shown).

TGF-β signaling does not affect initial import of Smad2. We next investigated whether TGF-β signaling also affected Smad import. This was achieved by bleaching whole nuclei of EGFP-Smad2-expressing cells and observing import of unbleached EGFP-Smad2 from the cytoplasm. Values were normalized to expression levels in each cell. At early time points, import kinetics did not differ significantly, irrespective of the absence or presence of a signal (Fig. 5Bi), indicating that phosphorylated EGFP-Smad2 is not imported more rapidly than unphosphorylated Smad2. However, differences did arise at later time points (Fig. 5Bii). For cells that are not stimulated with TGF-β, the import curves reached a plateau due to the establishment of a steady state between import and export after approximately 3 min (see also Fig. 3Ai). In contrast, the import curves for TGF-β-treated cells did not plateau, because these curves are made up of two contributions. At early time points, rapid import of unphosphorylated and phosphorylated EGFP-Smad2 is observed. At later time points, when the rapid exchange of unphosphorylated Smad2 has reached steady state, a sustained increase that is due to accumulation of phosphorylated EGFP-Smad2 becomes apparent. As discussed above, the rate of this slow increase in nuclear fluorescence is dictated by a slow phosphorylation rate rather than by fast translocation rate. Initial import rates of stably expressed EGFP-Smad2 in the absence and presence of TGF-β were also measured in a second cell line, HeLa TK$^-$ (1), with similar results (see Fig. S3 in the supplemental material).

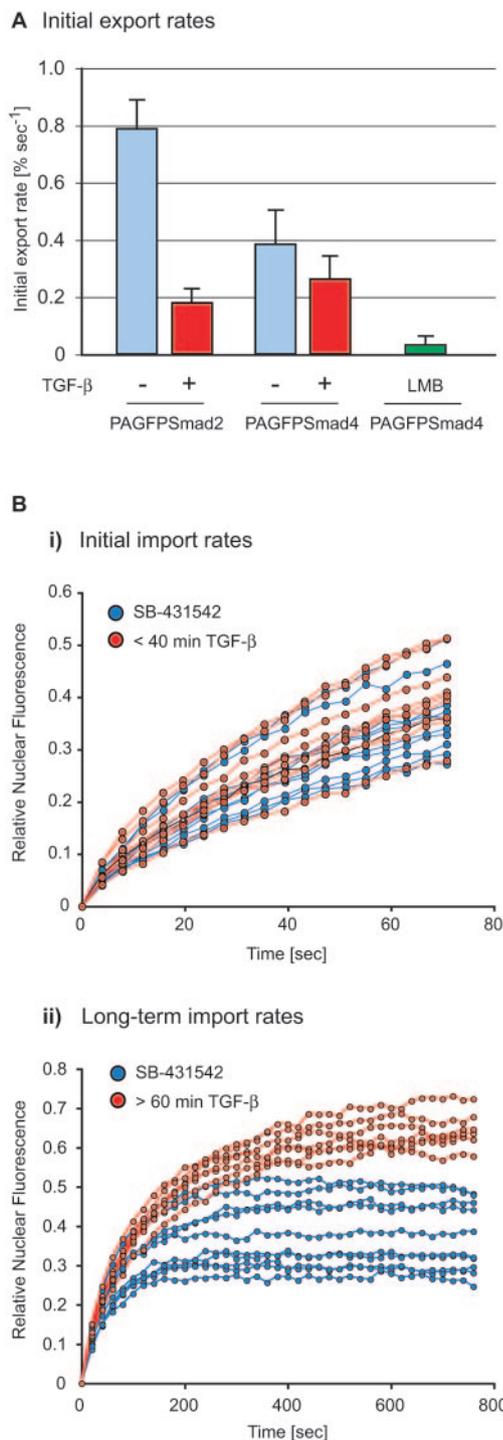From these experiments we conclude that Smad2 accumulation in response to TGF-β is not due to increased import,

orescence intensities of the nucleus (F_n) and the cytoplasm (F_c) were measured and the fluorescence ratio R was calculated. Bars show means ± standard deviations, n was 30 for each condition. C. Using R and an average ratio A between accessible cytoplasmic and accessible nuclear volume of 2.9 as obtained from kinetic experiments (Fig. 3 and Fig. S1 in the supplemental material), relative amounts of EGFP-Smad in the cytoplasm and nucleus of uninduced cells were calculated. Moreover, we estimated the relative fraction of EGFP-Smad that is nuclear in response to TGF-β. For details see the text. Values are given as a percentage of total cellular EGFP-Smad.

A Initial export rates

B

i) Initial import rates

ii) Long-term import rates

since the initial import rate is unchanged in the absence and presence of TGF-β.

Nuclear Smad mobilities change in response to TGF-β. Our results indicate that active Smad complexes are efficiently retained in the nucleus. We explored this further using fluorescence recovery after photobleaching (FRAP) to compare Smad mobilities in both the nucleus and cytoplasm.

FRAP experiments were performed in EGFP-Smad2- and EGFP-Smad4-expressing cells treated with either SB-431542 or TGF-β, and in the case of EGFP-Smad4, also LMB. As a control we measured FRAP of unfused PAGFP which is assumed to be freely diffusing. Representative FRAP curves averaged from 10 cells are shown (Fig. 6A and B). To show that the results are not cell type specific, we additionally carried out similar experiments in HeLa TK⁻ cells stably expressing EGFP-Smad2 (see Fig. S3 in the supplemental material).

Several important conclusions can be drawn from the FRAP curves. Firstly, even in the absence of TGF-β, the EGFP-Smad fusions were much less mobile than unfused PAGFP (Fig. 6A). This effect was much more pronounced than would be expected from the obvious size difference of the proteins (18), indicating that the Smads must be involved in binding reactions. Second, TGF-β causes a decrease in mobility in the nucleus, whereas accumulation of monomeric EGFP-Smad4 after treatment with LMB did not significantly affect the mobility of EGFP-Smad4 in the nucleus (Fig. 6A, right-hand panel). Thus, TGF-β-induced complex formation must be the cause of the observed differences in nuclear mobility, and these differences are not the result of higher nuclear Smad concentration. Hence, we conclude that phosphorylation and complex formation of Smads increases their affinity for nuclear binding sites, and this could be responsible for the decrease in export rate that we observe (Fig. 5A). In stark contrast to the FRAP results obtained in the nucleus, TGF-β does not change the mobility of the EGFP-Smads in the cytoplasm at all (Fig. 6B). We conclude that TGF-β does not cause a release of Smads from cytoplasmic tethering.

We quantitatively compared the FRAP curves by using recovery half-times, which give a reasonable estimation of the observed differences in mobility of the EGFP-Smad fusions in different conditions. Stimulation of cells with TGF-β has a substantial effect on recovery half-time for EGFP-Smad2, and a similar, but smaller effect on recovery half-time for EGFP-Smad4 (Fig. 6C). This difference between EGFP-Smad2 and EGFP-Smad4 is expected as EGFP-Smad4 accumulates in the nucleus less well than EGFP-Smad2 in response to TGF-β and much of the nuclear EGFP-Smad4 is nuclear due to constitutive shuttling of monomeric EGFP-Smad4. In fact, as discussed above, in TGF-β-treated cells approximately 80% of the nuclear EGFP-Smad2 is engaged in Smad complexes, while just over half of the nuclear EGFP-Smad4 is complexed. It is

FIG. 5. TGF-β stimulation affects the export rate of the Smads, but not the import rate. A. Cell lines expressing PAGFP-Smad2 and PAGFP-Smad4 were treated for 1 h as indicated and entire nuclei were photoactivated for 5 to 10 seconds. Loss of nuclear fluorescence due to export was monitored for 60 seconds after photoactivation. Data were normalized to the initial nuclear fluorescence directly after photoactivation and an initial export rate was obtained. Bars represent mean values and standard deviations obtained from 20 cells for each condition. Note that the export rate for Smad2 in unstimulated cells agrees well with the export rate constant obtained in Fig. 3. B. Nuclear import. Entire nuclei of EGFP-Smad2 cells were photobleached. Nuclear fluorescence immediately after the bleach was set to zero and reappearance of nuclear fluorescence was measured. Values were nor-

malized for expression levels, each curve represents a single cell. (i) Initial nuclear import in SB-431542-treated cells (blue curves) and cells treated with TGF-β for between 10 and 40 min, i.e., during the actual accumulation phase before establishment of a steady state (red curves). (ii) Nuclear import in cells treated for 1 h with SB-431542 (blue curves) and cells treated for 1 h with TGF-β and hence having reached a steady state of nuclear accumulation (red curves).
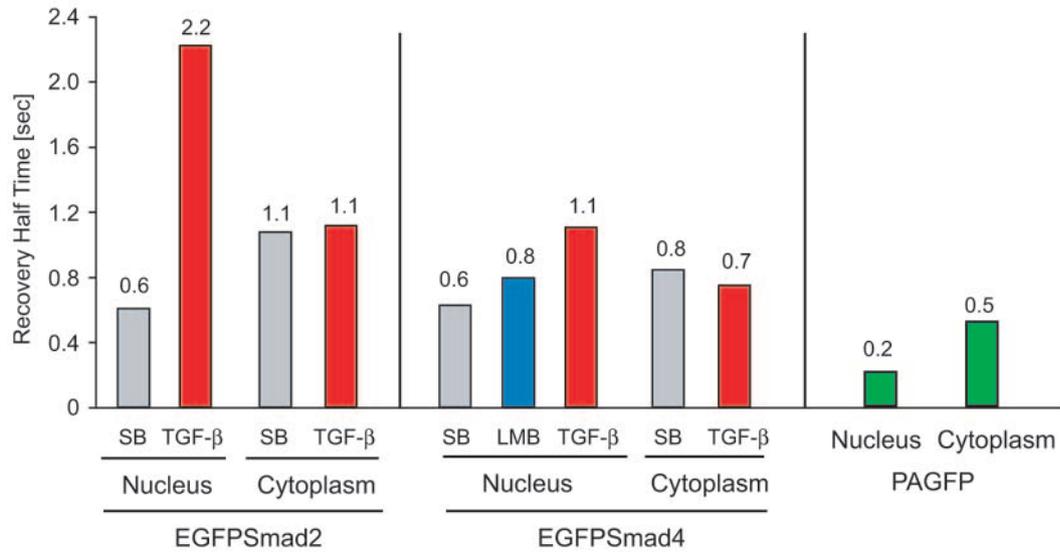
A   Nuclear FRAP
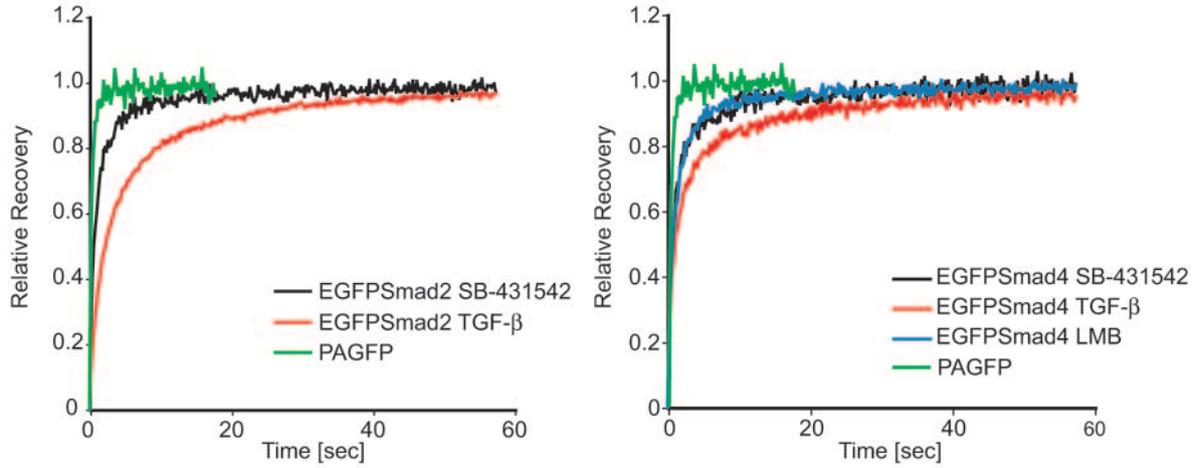
B   Cytoplasmic FRAP
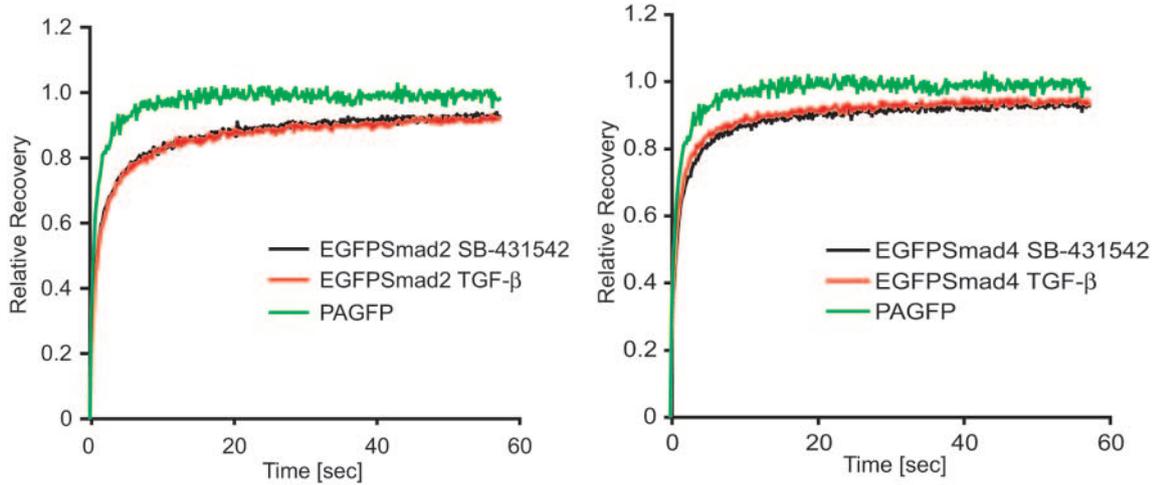
C   Recovery Half-Time

also clear from the recovery half-times that TGF-β has no effect on Smad mobility in the cytoplasm, although we do observe that the EGFP-Smads are slightly less mobile in the cytoplasm than in the nucleus (Fig. 6C). It is important to note that the recovery half-times only take into account the initial recovery phase. Differences in the FRAP curves however persist throughout the recovery. We find that the curves are complex and to achieve a good fit we require the sum of at least three exponentials (data not shown).

We attempted to identify the mechanism responsible for the decrease in mobility of the Smads in the nucleus in response to TGF-β. It has previously been suggested that interaction of the Smads with nuclear transcription factors such as Fast-1/FoxH1 could be responsible for retaining activated Smads in the nucleus (26). Indeed, overexpression of Fast-1/FoxH1 in HeLa TK⁻ cells stably expressing EGFP-Smad2 led to nuclear accumulation of EGFP-Smad2 in the absence of TGF-β (see Fig. S3C in the supplemental material). In such cells, the nuclear mobility of EGFP-Smad2 was dramatically decreased (see Fig. S3D in the supplemental material). This experiment demonstrates that Smad-interacting proteins with strong DNA-binding activity can recruit Smad2 into the nucleus when they are highly overexpressed, and can bring about a strong decrease in the mobility of Smad2, presumably by tethering it to DNA.

To test whether this sort of mechanism is indeed responsible for decreasing the nuclear mobility of EGFP-Smad2 upon TGF-β treatment, we generated an EGFP-Smad2 point mutant (W368A) that cannot interact with Fast-1/FoxH1 family members or with other transcription factors that contain the Smad interaction motifs defined in this family of transcription factors (14, 15; data not shown). This mutant Smad2 was efficiently phosphorylated in response to TGF-β, formed complexes with endogenous Smad2 and accumulated in the nucleus as efficiently as wild-type EGFP-Smad2 (see Fig. S2 in the supplemental material). Moreover, it showed a similar decrease in mobility in the nucleus upon TGF-β stimulation as seen by the FRAP curves and the recovery half-times (see Fig. S2 in the supplemental material). Thus, interaction of activated Smads with transcription factors such as Fast-1/FoxH1 does not account for nuclear accumulation or decreased nuclear mobility of Smad2 in response to TGF-β. However, the results that we obtain after overexpression of Fast-1/FoxH1 do suggest that interaction of EGFP-Smad2 with DNA could be responsible for the decreased nuclear mobility of EGFP-Smad2 we observe in TGF-β-treated cells.

In summary, our FRAP experiments indicate that TGF-β decreases the mobility of Smads in the nucleus, but has no effect on Smad mobility in the cytoplasm. Therefore, nuclear accumulation of the Smads in response to TGF-β likely involves an increased affinity of Smad complexes for nuclear

binding sites, and does not occur through release from cytoplasmic tethering.

DISCUSSION

Proposed mechanistic model. We have used compartment-specific photoactivation of PAGFP-Smads and bleaching of EGFP-Smads to provide direct evidence for Smad2 nucleocytoplasmic shuttling in real time in vivo, to observe Smad2 export independently of import and to determine the import and export rate constants for Smad2. This approach, complemented by FRAP studies, has yielded a quantitative analysis of the nucleocytoplasmic distribution of the Smads, which has given us novel insights into the mechanism of the TGF-β response.

We have shown that the predominantly cytoplasmic localization of Smad2 in unstimulated cells is due to Smad2 export being faster than Smad2 import. We have identified a pronounced decrease in nuclear export of TGF-β-activated Smad2 as the driving force of signal-induced nuclear accumulation of Smad2. We have correlated this finding both with the amount of activated Smad2 that accumulates in the nucleus in response to TGF-β, and with a TGF-β-induced decrease in Smad2 and Smad4 nuclear mobility. From these findings, we propose the following mechanistic model to explain the nuclear accumulation of Smads in response to TGF-β (Fig. 7).

In uninduced cells cytoplasmic Smad2 is continuously imported into the nucleus, but stronger constitutive export establishes a predominantly cytoplasmic localization. In agreement with the work of others we find that the C-terminal MH2 domain and linker region, which are present in our EGFP-Smad2 ΔMH1 mutant, are sufficient for both Smad2 import and export (25, 26). However, EGFP-Smad2 ΔMH1 does not show the correct subcellular localization in the cell, as unlike endogenous Smad2, it is substantially nuclear. We show that attenuation of Smad2 import by the MH1 domain is important for establishing a Smad2 subcellular localization that is predominantly cytoplasmic. We find that the nuclear import of EGFP-Smad2 is in fact very inefficient and is even lower than that for unfused PAGFP, which is thought to translocate through the nuclear pore by diffusion (16).

TGF-β-induced phosphorylation of Smad2 does not enhance this very inefficient import. In fact, increasing the import rate would be without effect on nuclear accumulation as the process of Smad2 phosphorylation is rate-limiting and considerably slower than Smad2 translocation into the nucleus (see below). Hence, per time interval, only a small percentage of the translocating Smad2 is actually phosphorylated. However, whereas unphosphorylated Smad2 is reexported by an unknown transport mechanism, phosphorylated, complexed Smad2 is retained in the nucleus. Increased affinity for nuclear binding

---

FIG. 6. Assessment of Smad mobilities in the nucleus and cytoplasm by FRAP. FRAP was performed on EGFP-Smad2- and EGFP-Smad4-expressing cells treated for 1 h with SB-431542 (SB), TGF-β or LMB. The curves represent data from 10 cells in each case. A. Nuclear recovery curves for EGFP-Smad2 (left panel) and EGFP-Smad4 (right panel). For comparison, the much faster recovery of photoactivated PAGFP, which is thought to be exclusively due to diffusion is shown. B. Cytoplasmic recovery curves of EGFP-Smad2 (left panel) and EGFP-Smad4 (right panel) in cells treated as indicated. Recovery of photoactivated PAGFP is shown for comparison. C. Recovery half-times, i.e., time after which the corresponding recovery curve has reached 0.5.
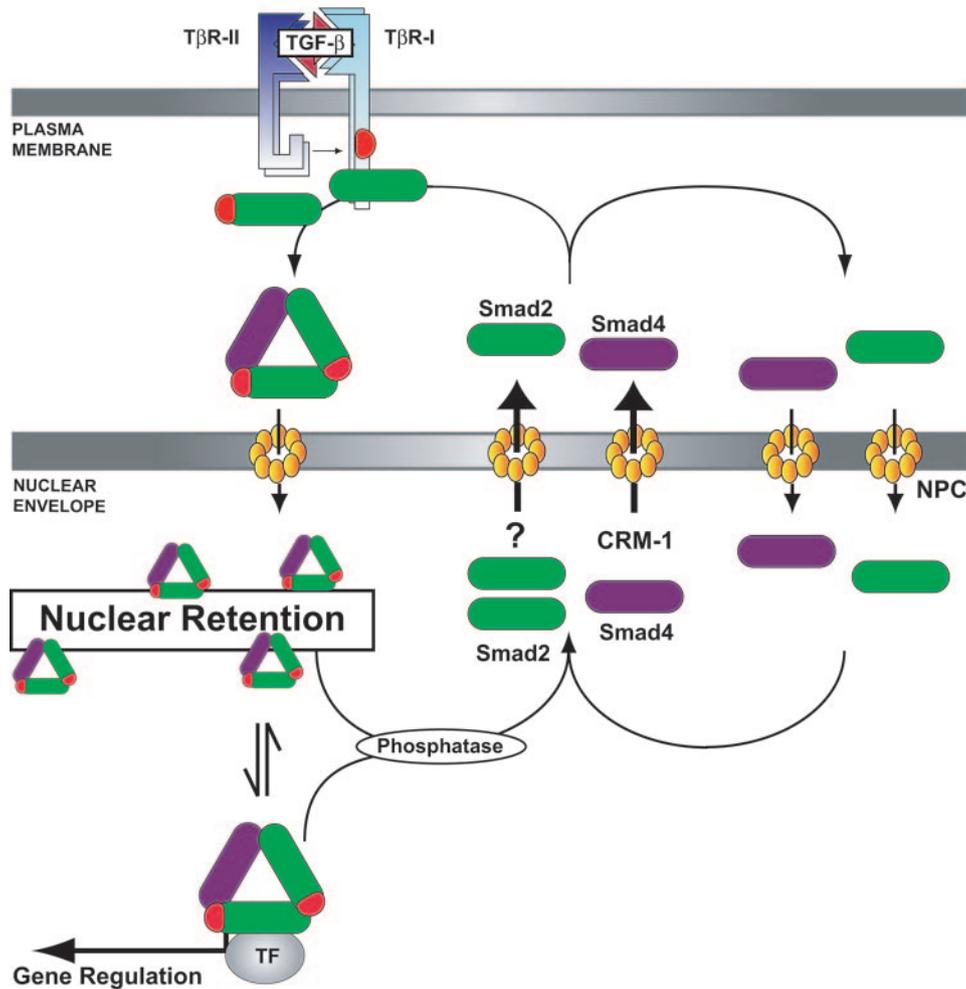
FIG. 7. Schematic model of Smad nucleocytoplasmic transport. For details, refer to the text. Red oval, phosphate group. NPC, nuclear pore complex. TF, transcription factor. TβR-I, TGF-β receptor type I. TβR-II, TGF-β receptor type II.

sites is most likely involved in this retention. Smad4 accumulation is a direct consequence of Smad2 accumulation. The pool of retained Smad complexes is in equilibrium with the presumably small fraction of Smad complexes that are actually engaged on specific target gene promoters. We postulate that in TGF-β-treated cells, weak phosphatase activity triggers dissociation of phospho-Smad2/Smad4 and phospho-Smad2/phospho-Smad2 complexes, enabling the monomeric subunits to be exported from the nucleus independently of each other. If the receptors are still active, Smad2 becomes rephosphorylated and reenters the accumulation cycle. Hence, the nucleus acts as a trap, filtering phosphorylated complexed Smad2 from the total shuttling pool, which eventually leads to nuclear accumulation. The actual speed and degree of nuclear accumulation are then determined by the relative rates of R-Smad phosphorylation and dephosphorylation.

There is no cytoplasmic pool of phosphorylated Smad2. Several lines of evidence suggest that there is no substantial pool of phosphorylated Smad2 in the cytoplasm at any time during active signaling. First, Smad2 emerging from the nucleus in TGF-β-treated cells is unphosphorylated (7, 26). Second, phosphorylation kinetics match nuclear accumulation ki-

netics, both reaching a maximum after ~45 min of TGF-β treatment (7, 10). Third, in TGF-β-stimulated cells in which Smad2 has reached a steady state and is predominantly nuclear, ongoing receptor activity is still required for strong accumulation of cytoplasmically photoactivated PAGFP-Smad2 (Fig. 2B), suggesting that cytoplasmic Smad2 is unphosphorylated in such cells. Fourth, a substantial pool of cytoplasmic phosphorylated EGFP-Smad2 would be expected to cause a difference in the cytoplasmic recovery curves in induced and uninduced cells, due to different sizes and binding properties of complexed versus monomeric Smads. However, TGF-β does not influence cytoplasmic mobility of EGFP-Smad2 at all, and the cytoplasmic FRAP curves for Smad2 in uninduced and TGF-β-induced cells superimpose (Fig. 6).

We conclude that there is no pool of phosphorylated EGFP-Smad2 in the cytoplasm, which indicates that translocation into the nucleus is much faster than phosphorylation. Hence, the phosphorylation rate or perhaps events upstream of phosphorylation will determine the rate of nuclear accumulation of phosphorylated Smad2. The speed of the actual translocation step is not rate limiting and therefore does not dictate the kinetics of the accumulation process.

TGF-β signaling regulates the export rate but not the import rate of Smad2. We have measured the initial import and export rates for EGFP-Smad2 in the absence and presence of TGF-β. We find that TGF-β regulates export rate, inducing an approximately fourfold decrease compared to the rate measured for constitutively shuttling EGFP-Smad2. In contrast, TGF-β has no effect on import rate. Hence, a decrease in export rate causes the nuclear accumulation of Smad2 in response to TGF-β. We do not think that this decrease in export rate in response to TGF-β reflects a decrease in translocation rate across the nuclear pore. Rather, it can be explained if we assume that only monomeric unphosphorylated Smad2 is capable of export; the phosphorylated complexed Smad2 being trapped in the nucleus (see below).

TGF-β treatment decreases the mobility of nuclear Smads, but has no effect on Smad mobility in the cytoplasm. We have used FRAP to demonstrate that TGF-β treatment strongly decreases the mobility of EGFP-Smads in the nucleus, but not in the cytoplasm. Cytoplasmic anchoring has been suggested to be an important factor in maintaining cytoplasmic localization, and release from such anchoring has been thought to be important for TGF-β-induced nuclear accumulation of Smads (24, 27). However we find no evidence for strong tethering in the cytoplasm and we detect no entirely immobile fraction of EGFP-Smads, either in the cytoplasm or in the nucleus as determined by bleach-rebleach experiments (data not shown). Instead, for EGFP-Smad2, we observe that nuclear export is faster than nuclear import in unstimulated cells. Thus, we favor the idea that this is the main driving force for establishing cytoplasmic localization of the Smads in uninduced cells. Furthermore, we see no effect on Smad mobility in the cytoplasm in response to TGF-β, suggesting that TGF-β-dependent release from cytoplasmic retention is not required for nuclear accumulation of the Smads in response to TGF-β.

In the nucleus, TGF-β induces a strong decrease in the mobilities of both EGFP-Smad2 and EGFP-Smad4. The correlation between decreased export and increased nuclear binding affinities for active Smad complexes strongly suggests a role for nuclear tethering in impairing export in response to TGF-β. However, the possibility that complexed Smads are simply not recognized by the export machinery is also plausible. In fact this has been recently demonstrated for Smad4, since complex formation with phosphorylated Smad3 precludes Smad4's interaction with its nuclear exporter, CRM-1 (2). At present we cannot test whether this is also the case for Smad2, as we do not know the nuclear exporter for Smad2.

We have investigated the mechanism that underlies the decrease in mobility in the nucleus upon TGF-β stimulation. We have shown that overexpression of the transcription factor Fast-1/FoxH1 in unstimulated cells can cause both nuclear accumulation and a strong decrease in nuclear mobility of EGFP-Smad2 in the absence of TGF-β. We assume that this overexpressed transcription factor is tethering the monomeric Smad2 to DNA and that this causes the decrease in nuclear mobility. Thus, DNA is a possible candidate for providing nuclear binding sites (10). The impaired mobility cannot be attributed to the comparably few DNA-bound transcriptionally active complexes present in an induced nucleus (5), but rather might reflect a nonspecific DNA scanning process of active Smad complexes.

Activated Smad2 can interact with DNA through a number of different mechanisms: through interaction with Smad4, through interaction with transcription factors such as the FoxH1 family members that contain the SIM and FM Smad interaction motifs (15), and through interactions with other transcription factors via different interaction motifs. We have shown that the Smad2 mutant W368A, which is deficient in interaction with FoxH1 family members, accumulates in the nucleus as efficiently as wild-type Smad2 and shows a similar decrease in nuclear mobility in response to TGF-β. Hence, abolishing interaction with transcription factors such as Fast-1/FoxH1 and others that contain the same Smad binding motifs is not sufficient to abolish the nuclear accumulation of Smad2. However, this mutant Smad2 might be recruited to DNA via other mechanisms. Further work is required to establish whether DNA binding of active Smad complexes is responsible for the TGF-β-dependent decrease in nuclear mobility of the Smads that we observed.

In summary, our kinetic analysis of Smad nucleocytoplasmic shuttling has allowed us to define the mechanism that determines the predominant cytoplasmic localization of Smad2 in uninduced cells, and we have demonstrated that it is a decrease in nuclear export of activated Smad2 complexes that accounts for nuclear accumulation in response to TGF-β. We have now obtained a wealth of quantitative data that describe Smad nucleocytoplasmic shuttling, and in the future will use it to build a kinetic model that can be used to predict the behavior of the system under different experimental conditions.

REFERENCES

1. **Angel, P., I. Baumann, B. Stein, H. Delius, H. J. Rahmsdorf, and P. Herrlich.** 1987. 12-O-Tetradecanoyl-phorbol-13-acetate induction of the human collagenase gene is mediated by an inducible enhancer element located in the 5′-flanking region. Mol. Cell. Biol. **7:**2256–2266.
2. **Chen, H. B., J. G. Rud, K. Lin, and L. Xu.** 2005. Nuclear targeting of TGF-β-activated Smad complexes. J. Biol. Chem. **280:**21329–21336.
3. **De Bosscher, K., C. S. Hill, and F. J. Nicolás.** 2004. Molecular and functional consequences of Smad4 C-terminal missense mutations in colorectal tumour cells. Biochem. J. **379:**209–216.
4. **Germain, S., M. Howell, G. M. Esslemont, and C. S. Hill.** 2000. Homeodomain and winged-helix transcription factors recruit activated Smads to distinct promoter elements via a common Smad interaction motif. Genes Dev. **14:**435–451.
5. **Hager, G. L., C. Elbi, and M. Becker.** 2002. Protein dynamics in the nuclear compartment. Curr. Opin. Genet. Dev. **12:**137–141.
6. **Inman, G. J., F. J. Nicolás, J. F. Callahan, J. D. Harling, L. M. Gaster, A. D. Reith, N. J. Laping, and C. S. Hill.** 2002. SB-431542 is a potent and specific inhibitor of Transforming Growth Factor-β superfamily type I activin receptor-like kinase receptors, ALK4, ALK5 and ALK7. Mol. Pharmacol. **62:**65–72.
7. **Inman, G. J., F. J. Nicolás, and C. S. Hill.** 2002. Nucleocytoplasmic shuttling of Smads 2, 3 and 4 permits sensing of TGF-β receptor activity. Mol. Cell **10:**283–294.
8. **Kurisaki, A., S. Kose, Y. Yoneda, C. H. Heldin, and A. Moustakas.** 2001. Transforming growth factor-β induces nuclear import of Smad3 in an importin-β1 and Ran-dependent manner. Mol. Biol. Cell **12:**1079–1091.
9. **Laping, N. J., E. Grygielko, A. Mathur, S. Butter, J. Bomberger, C. Tweed,**

J. Fornwald, R. Lehr, J. D. Harling, L. M. Gaster, J. F. Callahan, and B. A. Olson. 2002. Inhibition of transforming growth factor (TGF)-β1-induced extracellular matrix with a novel inhibitor of the TGF-β type I receptor kinase activity. Mol. Pharmacol. **62:**58–64.

10. **Nicolás, F. J., K. De Bosscher, B. Schmierer, and C. S. Hill.** 2004. Analysis of Smad nucleocytoplasmic shuttling in living cells. J. Cell Sci. **117:**4113–4125.

11. **Nicolás, F. J., and C. S. Hill.** 2003. Attenuation of the TGFβ-Smad signaling pathway in pancreatic tumor cells confers resistance to TGFβ-induced growth arrest. Oncogene **22:**3698–3711.

12. **Patterson, G. H., and J. Lippincott-Schwartz.** 2002. A photoactivatable GFP for selective photolabeling of proteins and cells. Science **297:**1873–1877.

13. **Pierreux, C. E., F. J. Nicolás, and C. S. Hill.** 2000. Transforming growth factor β-independent shuttling of Smad4 between the cytoplasm and nucleus. Mol. Cell. Biol. **20:**9041–9054.

14. **Randall, R. A., S. Germain, G. J. Inman, P. A. Bates, and C. S. Hill.** 2002. Different Smad2 partners bind a common hydrophobic pocket in Smad2 via a defined proline-rich motif. EMBO J. **21:**145–156.

15. **Randall, R. A., M. Howell, C. S. Page, A. Daly, P. A. Bates, and C. S. Hill.** 2004. Recognition of phosphorylated-Smad2-containing complexes by a novel Smad interaction motif. Mol. Cell. Biol. **24:**1106–1121.

16. **Ribbeck, K., and D. Gorlich.** 2001. Kinetic analysis of translocation through nuclear pore complexes. EMBO J. **20:**1320–1330.

17. **Shi, Y., and J. Massagué.** 2003. Mechanisms of TGF-β signaling from cell membrane to the nucleus. Cell **113:**685–700.

18. **Sprague, B. L., and J. G. McNally.** 2005. FRAP analysis of binding: proper and fitting. Trends Cell. Biol. **15:**84–91.

19. **Swanson, J. A., M. Lee, and P. E. Knapp.** 1991. Cellular dimensions affecting the nucleocytoplasmic volume ratio. J. Cell. Biol. **115:**941–948.

20. **Watanabe, M., N. Masuyama, M. Fukuda, and E. Nishida.** 2000. Regulation of intracellular dynamics of Smad4 by its leucine-rich nuclear export signal. EMBO Rep. **1:**176–182.

21. **Wu, J. W., R. Fairman, J. Penry, and Y. Shi.** 2001. Formation of a stable heterodimer between Smad2 and Smad4. J. Biol. Chem. **276:**20688–20694.

22. **Xiao, Z., R. Latek, and H. F. Lodish.** 2003. An extended bipartite nuclear localization signal in Smad4 is required for its nuclear import and transcriptional activity. Oncogene **22:**1057–1069.

23. **Xiao, Z., X. Liu, and H. F. Lodish.** 2000. Importin β mediates nuclear translocation of Smad3. J. Biol. Chem. **275:**23425–23428.

24. **Xu, L., C. Alarcon, S. Col, and J. Massagué.** 2003. Distinct domain utilization by Smad3 and Smad4 for nucleoporin interaction and nuclear import. J. Biol. Chem. **278:**42569–42577.

25. **Xu, L., Y. G. Chen, and J. Massagué.** 2000. The nuclear import function of Smad2 is masked by SARA and unmasked by TGFβ-dependent phosphorylation. Nat. Cell. Biol. **2:**559–562.

26. **Xu, L., Y. Kang, S. Col, and J. Massagué.** 2002. Smad2 nucleocytoplasmic shuttling by nucleoporins CAN/Nup214 and Nup153 feeds TGFβ signaling complexes in the cytoplasm and nucleus. Mol. Cell **10:**271–282.

27. **Xu, L., and J. Massagué.** 2004. Nucleocytoplasmic shuttling of signal transducers. Nat. Rev. Mol. Cell. Biol. **5:**209–219.